



## CLINICAL RESEARCH ARTICLE

# Preterm infants variability in cerebral near-infrared spectroscopy measurements in the first 72-h after birth

Sarah E. Kolnik<sup>1</sup>✉, Rebecca Marquard<sup>2</sup>, Olivia Brandon<sup>1</sup>, Mihai Puia-Dumitrescu<sup>1</sup>, Gregory Valentine<sup>1</sup>, Janessa B. Law<sup>1</sup>, Niranjana Natarajan<sup>1,3</sup>, Manjiri Dighe<sup>4</sup>, Pierre D. Mourad<sup>5,6</sup>, Thomas R. Wood<sup>1</sup> and Ulrike Mietzsch<sup>1</sup>

© The Author(s), under exclusive licence to the International Pediatric Research Foundation, Inc 2023

**BACKGROUND:** Cerebral near-infrared spectroscopy is a non-invasive tool used to measure regional cerebral tissue oxygenation (rScO<sub>2</sub>) initially validated in adult and pediatric populations. Preterm neonates, vulnerable to neurologic injury, are attractive candidates for NIRS monitoring; however, normative data and the brain regions measured by the current technology have not yet been established for this population.

**METHODS:** This study's aim was to analyze continuous rScO<sub>2</sub> readings within the first 6–72 h after birth in 60 neonates without intracerebral hemorrhage born at ≤1250 g and/or ≤30 weeks' gestational age (GA) to better understand the role of head circumference (HC) and brain regions measured.

**RESULTS:** Using a standardized brain MRI atlas, we determined that rScO<sub>2</sub> in infants with smaller HCs likely measures the ventricular spaces. GA is linearly correlated, and HC is non-linearly correlated, with rScO<sub>2</sub> readings. For HC, we infer that rScO<sub>2</sub> is lower in infants with smaller HCs due to measuring the ventricular spaces, with values increasing in the smallest HCs as the deep cerebral structures are reached.

**CONCLUSION:** Clinicians should be aware that in preterm infants with small HCs, rScO<sub>2</sub> displayed may reflect readings from the ventricular spaces and deep cerebral tissue.

*Pediatric Research* (2023) 94:1408–1415; <https://doi.org/10.1038/s41390-023-02618-x>

**IMPACT:**

- Clinicians should be aware that in preterm infants with small head circumferences, cerebral near-infrared spectroscopy readings of rScO<sub>2</sub> displayed may reflect readings from the ventricular spaces and deep cerebral tissue.
- This highlights the importance of rigorously re-validating technologies before extrapolating them to different populations.
- Standard rScO<sub>2</sub> trajectories should only be established after determining whether the mathematical models used in NIRS equipment are appropriate in premature infants and the brain region(s) NIRS sensors captures in this population, including the influence of both gestational age and head circumference.

**INTRODUCTION**

Cerebral near-infrared spectroscopy (NIRS) is a widely used monitoring technology that offers the ability to monitor regional cerebral tissue oxygenation (rScO<sub>2</sub>), which is postulated to be an expression of cerebral oxygenation and cerebral blood flow (CBF).<sup>1</sup> The goal of cerebral NIRS technology is to offer non-invasive continuous monitoring of cerebral tissue oxygenation and extraction, providing clinicians with the prospect of real-time monitoring of the patient's physiological state.<sup>2–5</sup> Currently, cerebral NIRS monitoring is employed in many neonatal intensive care units (NICU) across the world.<sup>5–7</sup>

The technology used for cerebral NIRS was created for adult and pediatric populations; however, it is important to recognize that a large discrepancy exists between adult, pediatric, and neonatal

head circumferences (HCs) and tissue composition.<sup>8</sup> There exists a paucity of data and studies evaluating differences in HC and tissue composition when examining baseline rScO<sub>2</sub> in relation to gestational age (GA) of the neonate.<sup>9</sup> This relationship is particularly important when monitoring preterm infants. Although some normal ranges for rScO<sub>2</sub> during the first 72 h after birth in preterm infants at different GAs have been published, data on normative values remain limited.<sup>1,10,11</sup> It is, however, widely accepted that changes in an individual's own baseline rScO<sub>2</sub> values are associated with alterations in oxygenation and oxygen extraction.<sup>6,11–13</sup> Interestingly, the specific brain region(s) measured with existing NIRS technology have not been determined in preterm infants.<sup>4</sup> The NIR beam is assumed to follow a banana-shape path and measurement depth is thought to be

<sup>1</sup>Department of Pediatrics, Division of Neonatology, University of Washington School of Medicine, Seattle, WA, USA. <sup>2</sup>Elson S. Floyd College of Medicine, Spokane, WA, USA.

<sup>3</sup>Department of Neurology, Division of Child Neurology, University of Washington School of Medicine, Seattle, WA, USA. <sup>4</sup>Department of Radiology, University of Washington, Seattle, WA, USA. <sup>5</sup>Division of Engineering and Mathematics, School of STEM, University of Washington, Bothell, WA, USA. <sup>6</sup>Department of Neurological Surgery, School of Medicine, University of Washington, Seattle, WA, USA. ✉email: [sekolnik@uw.edu](mailto:sekolnik@uw.edu)

Received: 4 November 2022 Revised: 29 March 2023 Accepted: 6 April 2023

Published online: 3 May 2023

approximately at 50–67% of the distance between emitter and detector.<sup>1–4</sup> Currently available neonatal cerebral NIRS sensors measure at an assumed depth of approximately 1.5–2.5 cm, depending on the manufacturer and the type of sensor used.<sup>14–16</sup> The actual path length of the NIR beam, which scales with the depth of tissue sampled, remains unknown.<sup>17</sup> Neonatal probes are typically smaller and have a shorter emitter-detector distance compared to the adult sensors.<sup>7</sup> Since the distance is a fixed parameter, the underlying, corresponding brain region in neonates may differ simply due to their smaller HCs and curvatures. Lack of reliability between rScO<sub>2</sub> readings has been reported when comparing sensors with different emitter-detector distances and also with simple repositioning of the same sensor on the same neonate highlighting the difference and optical heterogeneity of the underlying tissue.<sup>18</sup> Furthermore, tissue maturation, water composition, protein content, lipid content, and vascularization all influence optic properties, and therefore, rScO<sub>2</sub> measurements are subject to rapid changes in the still-developing neonatal brain compared to an adult.<sup>19</sup>

The aim of this study is to evaluate continuous rScO<sub>2</sub> readings within the first 72 h after birth in preterm infants without overt neurologic injury and to determine whether these readings were altered by GA, HC, or different brain regions captured by the commercially available neonatal sensor of the INVOS™ 5100C system.

## METHODS

### Patient selection

This was an observational single-center cohort study of preterm infants born at ≤1250 g and/or ≤30 weeks' gestation and admitted following delivery to the University of Washington Medical Center NICU between May 2019 and May 2021. Exclusion criteria were <66 h of continuous rScO<sub>2</sub> monitoring, major congenital anomalies, death within 72 h after birth, HC >30 cm (Z-score >3), and intracranial hemorrhage (ICH) diagnosed by cranial ultrasound 7–10 days after birth as half of these hemorrhages are likely to have occurred by the first day of life.<sup>20</sup> The study was approved by the Institutional Review Board at the University of Washington School of Medicine UW IRB #0006091.

### Data collection

Demographic and clinical data collection occurred retrospectively from the medical record and included administration of prenatal corticosteroids, maternal pre-eclampsia, maternal chorioamnionitis, birth weight, GA, HC obtained within 1 h of birth (birth HC), next recorded HC after initial birth HC, small for GA defined as birth weight <10th percentile, Apgar score at 1 and 5 min after birth, respiratory support type at birth, first diastolic blood pressure after birth, first hematocrit, vasopressor use, and lowest and highest measured pCO<sub>2</sub> in the first 72 h after birth. For the first hematocrit, the value from the day of birth was used; if no value was available on day of birth, the value from day 1 after birth was used. For the first documented diastolic blood pressure, an arterial measurement was used; if no arterial measurement was available, a non-invasive measurement was utilized. Diastolic blood pressure was examined as CBF in preterm neonates has been shown to be highly reliant on diastolic blood flow.<sup>21</sup>

### NIRS monitoring and technology

Infants were monitored prospectively with continuous cerebral NIRS using the INVOS™ 5100C regional oximeter with INVOS cerebral oximetry infant-neonatal sensor (Medtronic, Minneapolis) during the first 72 h after birth. The infant-neonatal sensor has two detectors: a shallow detector spaced 3 cm from the emitter and a deep detector spaced 4 cm from the emitter. The shallow detector measures at a depth of approximately 1.5 cm, whereas the deep detector measures at a depth of approximately 2.5 cm. The measurement depth is derived using spatially resolved spectroscopy, subtracting shallow detector measurement from the deep detector measurement to remove the interference of measurements from superficial structures such as the skin, muscle, bone, and axial spaces, providing a reading at approximately 2.5 cm depth.<sup>14,22</sup> The infant-neonatal sensor was placed on the neonate's forehead within the first 6 h after birth. We chose to examine data from 6 h onward to best harmonize data analysis

across the entire cohort. rScO<sub>2</sub> data were captured in 5–10-s intervals and exported via INVOS™ Analytics Tool version 1.2.1 (Medtronic, Minneapolis).

### Measurements of fetal MRI

Fetal T2 MRI brain images were provided by the Harvard Fetal Brain Atlas ([http://crl.med.harvard.edu/research/fetal\\_brain\\_atlas/](http://crl.med.harvard.edu/research/fetal_brain_atlas/)), accessed March 15, 2022. Each image pixel represents an area of 0.8 mm<sup>2</sup>, allowing for an elliptical arch to be drawn corresponding with the infrared ray detector and arch depth measurements listed above. The depths of the rays were adjusted to account for scalp and skull depth, which in neonates and newborns has been measured as less than 1 mm.<sup>23</sup> As the path of the ray is influenced by multiple factors including myelination and water content of the structures through which the ray is passing, these arches are provided as estimates. Image analysis and measurements were performed using FMRIB Software Library (FSL v6.0, Oxford, UK, <https://fsl.fmrib.ox.ac.uk/fsl/fslwiki/FslInstallation>), accessed November 23, 2021.<sup>24–26</sup> Graphical illustration and coloring of the arches was performed using Microsoft PowerPoint (2019, Version 2211 Build 16.0.15831.20098).

### Statistical analysis

Descriptive statistics were used to describe the demographic variables of the included infants using either median and interquartile range (IQR) or count and percentage. rScO<sub>2</sub> data were averaged into hourly epochs by determining the median value for each infant in each epoch. To visually examine how rScO<sub>2</sub> changes with HC and GA, continuous rScO<sub>2</sub> curves were generated using locally estimated scatterplot "loess" fitting with either standard deviation (aggregated trajectories) or 95% confidence intervals (CI, individual patient trajectories) starting 6 h after birth. Trajectories of rScO<sub>2</sub> were plotted for three HC groups (18–21.9, 22–25.9, and ≥26 cm) and four GA groups (22–24, 25–27, 27–29, and ≥30 weeks). For GA plots, infants with an HC Z-score more than ±2 were excluded (*n* = 7). To examine the population effects of GA and HC on rScO<sub>2</sub> over time, a generalized estimating equations (GEE) approach was used.<sup>27</sup> Linear GEE models accounting for HC, GA, hematocrit, and time (as hourly epoch) were constructed, with clustering by infant and an exchangeable correlation structure. Both HC was modeled a third-order polynomial, with time epoch as a second-order polynomial and hematocrit and GA as linear continuous variables. A multivariate Wald test was used to compare models with and without the HC terms. Daily hematocrit was used and aligned with the respective epochs, with missing values replaced with the nearest available hematocrit level. Graphs of the data and their respective assumptions in the GEE model are provided in Supplementary Fig. S1. *P* values <0.05 were considered statistically significant. Statistical analyses were performed in R version 4.1.2 in the R studio environment.<sup>28</sup>

## RESULTS

During the study period, 98 infants were monitored with cerebral NIRS. Of those, we excluded 2 infants (2.0%) with congenital abnormalities, 3 infants (3.1%) with HCs >30 cm, 4 infants (4.1%) who died prior to 72 h of NIRS monitoring, and 30 infants (30.6%) who were diagnosed with ICH. The remaining 60 (61.2%) infants were included in our analysis (Fig. 1). Baseline characteristics of the study population are depicted in Table 1. Median (IQR) number of hours of data collection in the 60 infants was 66 (65.5–66), indicating that most infants had data for the entire 6–72 h period after birth. We found no significant difference between HC at birth (median 24.5 cm, IQR 23.4–26.5) and next measured HC (median 24.0 cm, IQR 23.0–25.95) (Supplementary Table S2 and Supplementary Fig. S2).

### Determination of estimated NIRS sensor measurement by head circumference and gestational age

First, we determined the anatomical structures located at a signal depth of 2.5 cm using a fetal MRI atlas as a reference guide for normal brain development. The anatomical structures captured 2.5 cm from the forehead, where the NIRS probe is placed, are listed in the table in Fig. 2a. Representative images in Fig. 2b depict the approximate trajectory of where the rScO<sub>2</sub> reading arises for a given HC—the red arc estimates the light path for the deep sensor and blue arc estimates the light path for the shallow

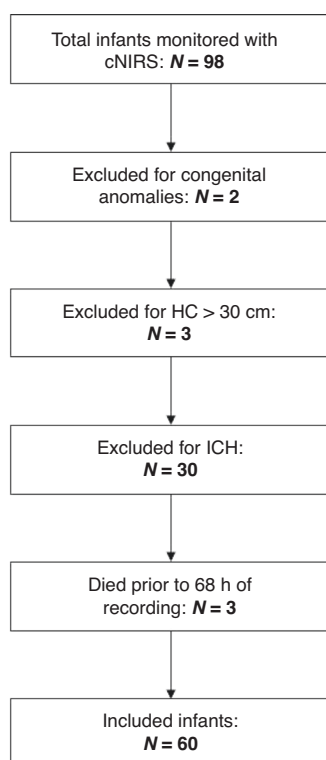


**Fig. 1 Consort diagram.** Screened and final infants included in this study are shown.

sensor. In infants with HC <30 cm, there is a high probability that at least a portion of the rScO<sub>2</sub> readings reflects data from ventricular cerebrospinal fluid (CSF). For infants with an HC <27 cm, the majority of the rScO<sub>2</sub> reading is likely to come from the ventricle and deep brain structures.

Based on the results in Fig. 2, infants were grouped by the anatomical structures estimated to be measured most frequently within a given HC and GA. This resulted in three groups for rScO<sub>2</sub> trajectory analysis as follows—Group 1: 18–21.9 cm with an estimated measurement level at the deep gray matter structures, Group 2: 22–25.9 cm with the estimated measurement of the cerebral NIRS sensor coming from the ventricle, and Group 3: 26–30 cm, with an estimated measurement region of cortex and white matter.

### rScO<sub>2</sub> in relation to head circumference and gestational age

The median rScO<sub>2</sub> trajectory over the first 6–72 h after birth varied significantly based on different HCs. Infants with the largest HC had the highest rScO<sub>2</sub> readings and average rScO<sub>2</sub> tended to decrease with decreasing HC (Fig. 3a).

Similar trajectories of rScO<sub>2</sub> were observed in relation to GA. The most immature infants had the lowest measured rScO<sub>2</sub> trajectories, whereas the more mature infants had higher rScO<sub>2</sub> measurements (Fig. 3b).

While the relationship between GA and rScO<sub>2</sub> was linear, HC was non-linearly associated with rScO<sub>2</sub> (Supplementary Fig. S1a, b). In particular, rScO<sub>2</sub> appeared to decrease with decreasing HC, but flattened or potentially began to increase again as HC decreased below 22 cm.

### Influence of gestational age on rScO<sub>2</sub> in infants with similar head sizes

To examine the role of changes in tissue composition with increasing GA on rScO<sub>2</sub> measurement, we grouped the neonates into two categories: Group 1 HC <26 cm, and Group 2 HC ≥26 cm. The two categories were derived by determining that those with HC

**Table 1.** Baseline patient characteristics.

	Participating infants (n = 60)
Birth weight (g)	877 (737–1101)
Gestational age <sup>a</sup> (completed weeks)	27 (22–33)
Head circumference <sup>a</sup> (cm)	24.5 (19–30)
Head circumference (Z-score)	−0.44 (−1.02 to 0.14)
Small for gestational age	17 (28.3%)
Prenatal corticosteroids	
None	5 (8.3%)
1 dose	9 (15.0%)
2+ doses	46 (76.7%)
Maternal pre-eclampsia	18 (30.0%)
Maternal chorioamnionitis	2 (3.3%)
Respiratory support type at birth	
CPAP	39 (65.0%)
Intubated	20 (33.3%)
Room air	1 (1.7%)
First diastolic blood pressure (mmHg)	29 (26–34)
Vasopressor use	4 (6.7%)
First hematocrit (%)	43 (40–49)
Apgar	
1 min	4 (3–5)
5 min	7 (6–7)
Apgar 5 min <5	5 (8.3%)
pCO <sub>2</sub> (mmHg) during first 72 h	
Lowest	39.3 (34.3–43.8)
Highest	57.6 (46.3–64.6)
Died after 72 h of life (without IVH)	2 (3.3%)

Median and interquartile ranges or count with percentages reported.

<sup>a</sup>Except for gestational age and head circumference as full range given.

≥26 cm likely had rScO<sub>2</sub> readings in part in the cortex (Fig. 2). As expected, higher GA was associated with higher rScO<sub>2</sub> measurements even after accounting for HC grouping (Fig. 3c, d); however, the range of rScO<sub>2</sub> measurements in neonates with HC <26 cm was 59–85% across all GAs compared to 76–87% in neonates with HC >26 cm, demonstrating a dominant effect of HC on rScO<sub>2</sub> measurement (Fig. 3c, d). Similarly with matched GA infants at 26 and 28 weeks, those with larger HC had higher rScO<sub>2</sub> measurements (Fig. 3e, f).

### After accounting for GA, HC also contributes to rScO<sub>2</sub> readings

In the fully adjusted GEE model, terms for HC, GA, and hematocrit were all significantly associated with the median rScO<sub>2</sub> value (Supplementary Table S1). Using a multivariate Wald test, the HC terms were statistically significant ( $p = 0.031$ ), suggesting that HC is an important contributor to rScO<sub>2</sub> after accounting for complex relationships with GA and time, as well as adjusting for hematocrit.

### DISCUSSION

As the field of neonatology continues to advance and the lower limit of viable GA continues to decrease, clinicians are faced with technologies that are not completely adapted or validated to their youngest patients. In the case of cerebral NIRS, this includes smaller head sizes which results in considerable variation in the brain region being measured by current cerebral NIRS sensors. To date, no studies have been conducted evaluating which

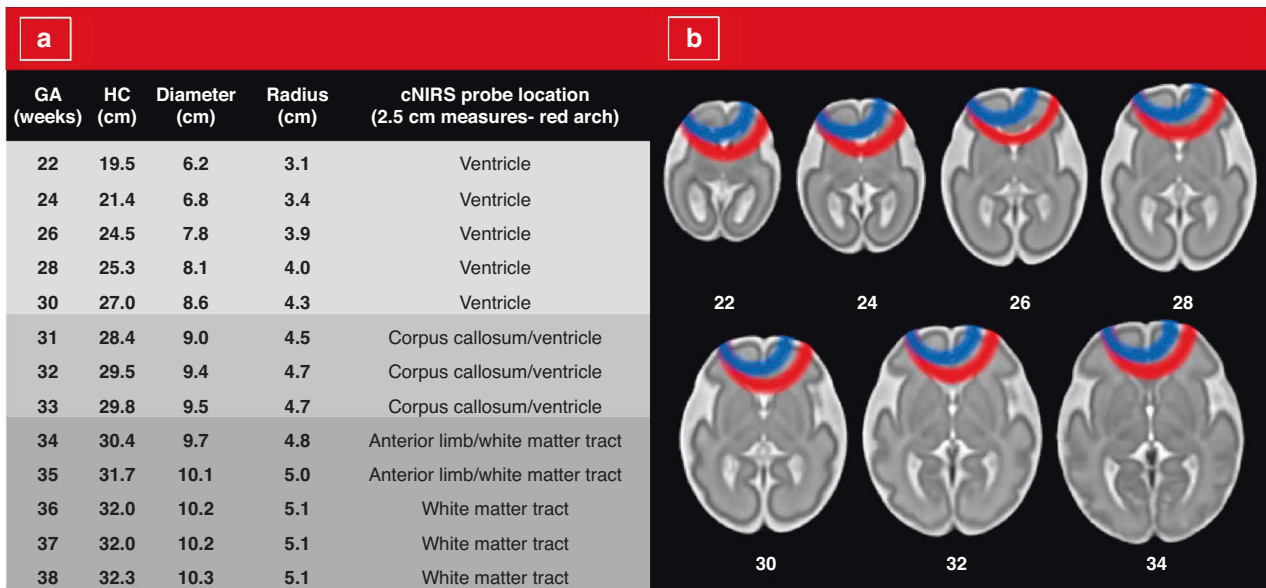


**Fig. 2** Estimated NIRS sensor measurement by head circumference and gestational age. **a** Head circumference and brain region captured by rScO<sub>2</sub> at 2.5 cm depth from midline forehead for increasing gestational ages (22–38 weeks gestation) as derived from fetal brain MRI images. For each head circumference, the diameter (head circumference/ $\pi$ ) is calculated for an assumed perfectly circular head shape and the radius (diameter/2) as well as the estimated brain structure in the presumed area. **b** Simulation of rScO<sub>2</sub> detection depths from the midline forehead overlying axial T2 fetal brain MRIs for increasing gestational ages as depicted in 22, 24, 26, 28, 30, 32, and 34 weeks of gestation. The blue and red arches represent the underlying areas captured by the short- and long-distance emitted infrared rays, respectively.

intracranial regions are measured by NIRS technology in preterm babies, or how rScO<sub>2</sub> values change over time. As rScO<sub>2</sub> readings are increasingly incorporated into clinical decision making, it is imperative to understand the brain region captured in preterm infants. In our study, we present rScO<sub>2</sub> trajectories over the first 6–72 h after birth in a cohort of 60 preterm infants born at  $\leq 1250$  g or  $< 30$  weeks gestation without ICH. We show that in these first 6–72 h, the expected rScO<sub>2</sub> trajectory is different when stratified by HC independent of GA, emphasizing the importance of the tissue being measured. In particular, rScO<sub>2</sub> readings in infants with HCs  $< 26$  cm are likely to have a higher proportion of the rScO<sub>2</sub> measurement by ventricular content, therefore not consistently reflecting cerebral tissue oxygenation itself (Fig. 2). In the smallest heads, rScO<sub>2</sub> may then incorporate greater proportions of deep gray matter, with independent non-linear effects of HC on rScO<sub>2</sub> after taking into account GA and hematocrit.

In a cerebral NIRS probe, light is detected by proximal and distal detectors, which allows for the processing of the shallow and deep optical signals separately to provide a spatial resolution; data from the scalp and surface tissue are subtracted and suppressed to provide a reading that reflects rScO<sub>2</sub> in deeper tissues.<sup>22,29–32</sup> Unlike the adult, pediatric, or even term newborn, the region of rScO<sub>2</sub> reading in preterm infants is unlikely to be the superficial cortex and may frequently extend through the ventricles into the deep gray matter (Fig. 2). For example, the average HC of term neonates is 35 cm with a radius of 5.5 cm (assuming a perfectly round head shape), and an average adult HC is 55 cm with a radius of 8.7 cm.<sup>33,34</sup> In our cohort, the smallest HC was 18 cm, which equates to a radius of 2.9 cm. Therefore, rScO<sub>2</sub> measurements reflect deeper cerebral structures rather than just the cortical white matter. Given that light absorption through the skull and extracerebral tissues is negligible in neonates, the NIR beam projects into the ventricles and deep gray matter.<sup>30,31</sup> The different anatomical structures of the brain also vary in composition. As an extreme example, CSF in the ventricles clearly has a different composition and oxygen content relative to white matter structures measured in larger HCs or deep gray matter structures measured in smaller HCs.<sup>19,32,35</sup> Although NIRS technology was

created to measure regional tissue oxygen bound to hemoglobin, CSF itself has been shown to alter the propagation of light in NIRS models.<sup>32,35–38</sup> Our results support the potential for CSF (or the absence of tissue) to interfere with the rScO<sub>2</sub> reading, with a greater proportion of CSF included at the 2.5 cm measurement depth in infants with smaller HCs (Fig. 2), which is associated with lower rScO<sub>2</sub> independently of GA (Fig. 3).

Despite the same wavelength, optical path length differs in adult and neonatal heads (average of 6.26 vs 4.99 cm, respectively) and can vary in the same subject with changes in tissue geometry, tissue water content, and hemoglobin concentration.<sup>29,39,40</sup> Tissue composition and myelin content change throughout neonatal developmental stages and also affect the brain's optical properties. For example, the penetration depth is highly dependent on the scattering effect of myelin which is not well developed in the extreme preterm brain; therefore, penetration depth of the emitting light might be even deeper than the expected 2.5 cm.<sup>19,41</sup> This process is dynamic, with myelination starting in the brainstem around 20 weeks of gestation and progressing rapidly alongside a concurrent decrease in ventricle size.<sup>19,42</sup> Furthermore, deep gray matter has differences in optical properties compared to white matter, which may account for further variations in rScO<sub>2</sub> based on the region of measurement.<sup>35</sup> Thus, not only is head size and physical location of the cerebral NIRS probe crucial when interpreting values, but the change of maturational tissue composition also needs to be considered when evaluating rScO<sub>2</sub> measurements over time.

The anatomical structures captured also vary in their vasculature and microvasculature, which results in a difference of the mixed arterial and venous signal for which the NIRS algorithm is engineered to report.<sup>43</sup> rScO<sub>2</sub> is calculated from the difference between arterial and venous oxygenation ( $fSO_2 = 0.25 \times SaO_2 + 0.75 \times SvO_2$ ), which changes with age.<sup>43</sup> While this 25:75 constant of arterial to venous blood is applicable to adults, pediatric patients have a constant of 15:85, and no normative values have been established in (preterm) neonates.<sup>43</sup> Furthermore, regional trends in rScO<sub>2</sub> at lower GAs differ from those of the peripheral vasculature, perhaps due to variations in the arterial:venous



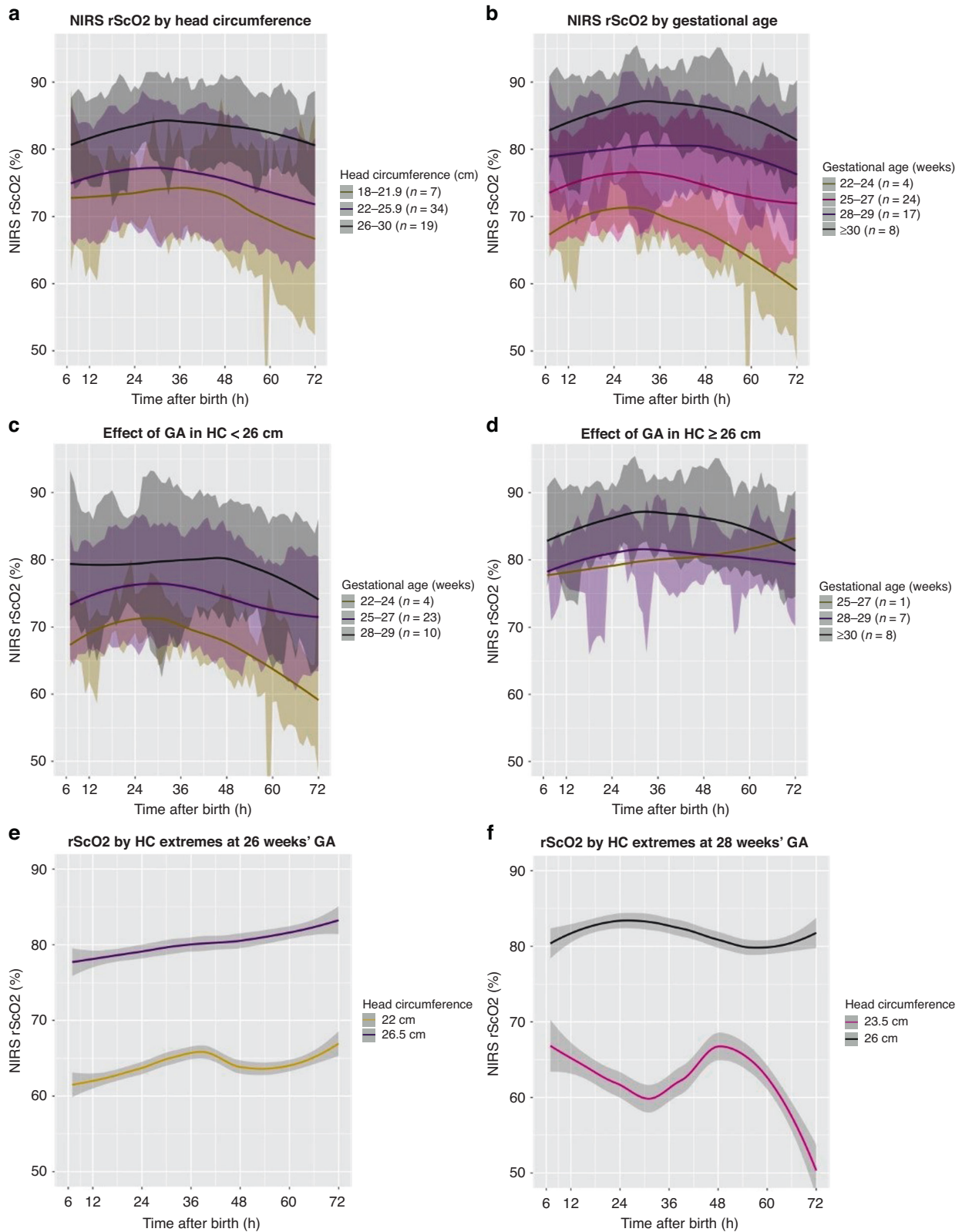


**Fig. 3** rScO<sub>2</sub> trajectories by head circumference and gestational age. **a** rScO<sub>2</sub> trajectories by head circumference (HC) stratified into numerical tertiles: 18–21.9, 22–25.9, and 26–30 cm. Larger HC demonstrates higher rScO<sub>2</sub> trajectories. **b** rScO<sub>2</sub> trajectories by gestational age at birth stratified into numerical quartiles: 22–24, 25–27, 27–30, and >30 weeks of gestation. More mature infants show higher rScO<sub>2</sub> trajectories. **c** rScO<sub>2</sub> trajectories of infants with HC <26 cm stratified by gestational ages into tertiles: 22–24, 25–27, and 27–30 weeks of gestation. **d** Cerebral NIRS rScO<sub>2</sub> trajectories of infants with HC ≥26 cm stratified by gestational ages in tertiles: 25–27, 27–30, and >30 weeks gestation. **e** rScO<sub>2</sub> at 26 weeks GA is higher in the neonate with larger HC. **f** rScO<sub>2</sub> at 28 weeks remains higher in the neonate with the larger HC compared to smaller HC. Trajectories were plotted using the locally estimated scatterplot smoothing (loess) method. Shaded areas indicate either the standard deviation (calculated hourly, **a–e**) or 95% CI (**e, f**).

constant in cerebral tissue.<sup>43</sup> The relatively larger proportion of venous volume at younger GAs may partially explain why cerebral rScO<sub>2</sub> values are lower in these infants and may be further exacerbated by differences in developmental stages of vascularization in the brain region measured.<sup>44</sup> For example, a recent study using pulse sequence MRI in neonates found that veins draining the central brain had 5% lower cerebral venous oxygenation (65% compared to 70%;  $p = 0.02$ ) than veins draining cortical brain.<sup>45</sup> This may provide an additional mechanistic explanation of how venous differences could help account for lower rScO<sub>2</sub> measurements in neonates with smaller HCs in whom the probe measures more centrally (Fig. 3b).

Lastly, fluctuations in cerebral arterial and venous volume in neonates are unique during the transitional period immediately following birth.<sup>43,46</sup> As depicted in Fig. 3, rScO<sub>2</sub> measurements increase around 12–14 h and peak at 24–30 h. These transitions in rScO<sub>2</sub> differ clinically from the peripheral venous saturation, which transitions and stabilizes within minutes after birth.<sup>47</sup> Changes in rScO<sub>2</sub> over time may result from a known transient decrease in arterial CBF after birth that then increases again by 24 h after birth.<sup>48</sup> In addition, if the arterial component is less than the empirically derived 25% by the INVOS technology, the decrease in the reading might be artifactual.<sup>14,22</sup> This alteration appears to be more pronounced at lower GAs, which is consistent with the inverse relationship between CBF autoregulation and GA.<sup>21,46,48,49</sup> The rScO<sub>2</sub> unique shape during the transitional period may also be accounted for by a GA-related decrease in vascular resistance and subsequent increase in venous circulation following delivery (Fig. 3).<sup>50</sup>

NIRS technology relies on light absorption by hemoglobin, using near-infrared light at wavelengths 730 and 810 nm to allow absorption by hemoglobin.<sup>22</sup> Furthermore, a higher hematocrit, has been positively correlated to rScO<sub>2</sub> readings in pediatric and neonatal patients.<sup>51–53</sup> In our model, hematocrit was positively correlated and thus accounted for when deciphering the HC and rScO<sub>2</sub> association (Supplementary Table S1 and Supplementary Fig. S1). Alderliesten et al. did not find an association between HC

and rScO<sub>2</sub> and thus postulated that differences in CBF account for the observed differences between infants of different GAs; however, their data did not account for the potential contribution of differing tissue type and composition nor did their study differentiate between infants with and without ICH.<sup>1</sup> Since NIRS probes in preterm infants may be capturing an area filled with CSF, blood within the CSF would be expected to alter rScO<sub>2</sub> as suggested by recent evidence.<sup>13,50,54</sup> Therefore, any studies of rScO<sub>2</sub> in premature infants must account for influence of intraventricular hemoglobin.<sup>55–58</sup> Lastly, although NIRS technology is designed to measure the concentration changes of oxy and deoxy-hemoglobin, the presence of hemoglobin has not been shown to be a requirement for getting a reasonable reading—it has been described that NIRS readings are still possible in metabolically inactive tissues from cadavers and objects void of hemoglobin such as vegetables.<sup>41,59</sup> The high prevalence of ICH in preterm infants, and the likelihood that a blood clot resulting from an ICH would be an important confounder when examining rScO<sub>2</sub> from infants with smaller HCs where readings include the ventricles, suggests that any studies of cerebral NIRS in premature infants must account for the impact of ICH.<sup>55–58</sup>

There are several limitations to this study including not knowing the exact location of the rScO<sub>2</sub> probe placement on each infants' forehead; however, as noted in the images, the depth of the signal will only have infrequently measured cortex regardless of where the probe was placed. Another limitation of this study is that rScO<sub>2</sub> measurements are multifactorial, thus isolating one contributory or causative factor is challenging.<sup>43</sup> We attempted to overcome overt contributions by excluding infants with ICH or congenital anomalies such as congenital heart disease, which is known to alter rScO<sub>2</sub> significantly.<sup>55,56</sup> However, due to the multitude of interrelated clinical factors that affect rScO<sub>2</sub> readings, future studies using matched time series will be required to accurately delineate the contributions of these factors independently (Fig. 4). Future studies evaluating a shortened distance between the light source and the receiver should be considered to determine whether more shallow

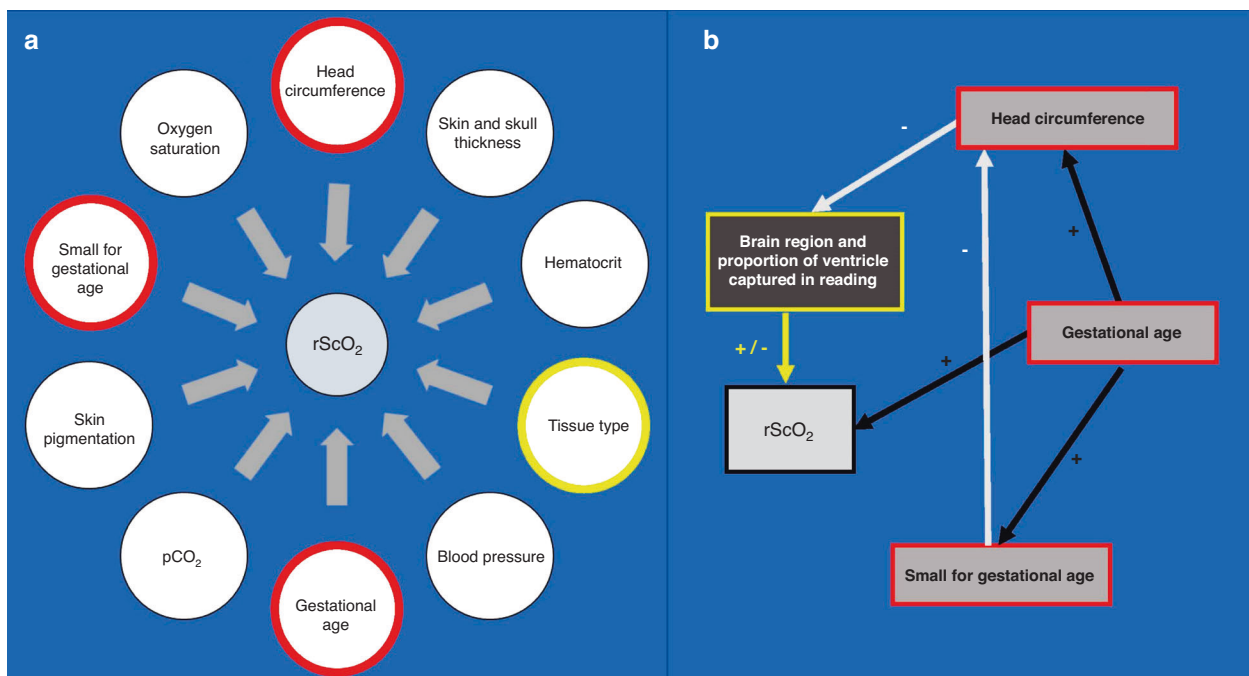


**Fig. 4** Factors that influence rScO<sub>2</sub> measurements. **a** Multitude of factors that have been shown to influence rScO<sub>2</sub> measurements. Factors outlined in red and yellow are addressed in this study. **b** Theoretical interrelated factors that affect cerebral NIRS measurements in this study. Light gray arrows depict a negative relationship. Black arrows depict a positive relationship. Yellow arrow depicts positive or negative relationship depending on where NIRS probe is capturing signal.

measurements result in more reliable rScO<sub>2</sub> from the cortex and more homogeneous readings across different GAs. If this is the case, this would support the development of a probe that was tailored to different HCs.

In summary, we objectively describe how HC and rScO<sub>2</sub> readings are positively but non-linearly correlated in preterm infants, which is likely due to variation in the brain region the cerebral NIRS probe is sensing at a fixed distance. Standard rScO<sub>2</sub> trajectories should only be established after determining (1) whether the mathematical models used in NIRS equipment are appropriate in premature infants, and (2) the brain region(s) that are captured by commercially available NIRS sensors in this population, including the influence of both GA and HC.

## DATA AVAILABILITY

The datasets generated and analyzed during the current study are available from the corresponding author on reasonable request. De-identified NIRS data are subject to an institutional data use agreement. Fetal T2 MRI brain images in the Harvard Fetal Brain Atlas are available online at [http://crl.med.harvard.edu/research/fetal\\_brain\\_atlas/](http://crl.med.harvard.edu/research/fetal_brain_atlas/).

## REFERENCES

- Alderliesten et al. Reference values of regional cerebral oxygen saturation during the first 3 days of life in preterm neonates. *Pediatr. Res.* **79**, 55–64 (2016).
- Vaidya, R. et al. Utilizing near infra-red spectroscopy to identify physiologic variations during digital retinal imaging in preterm infants. *J. Perinatol.* **42**, 378–384. <https://doi.org/10.1038/s41372-021-01294-1> (2022).
- Tataranno, M. L. et al. Early oxygen-utilization and brain activity in preterm infants. *PLoS One* **10**, e0124623 (2015).
- Vesoulis, Z. A., Mintzer, J. P. & Chock, V. Y. Neonatal NIRS monitoring: recommendations for data capture and review of analytics. *J. Perinatol.* **41**, 675–688 (2021).
- Pichler, G. et al. Cerebral regional tissue Oxygen Saturation to Guide Oxygen Delivery in preterm neonates during immediate transition after birth (COSGOD III): multicentre randomised phase 3 clinical trial. *BMJ* **380**, e072313 (2023).
- Chock, V. Y. et al. Cerebral oxygenation and autoregulation in preterm infants (Early NIRS Study). *J. Pediatr.* **227**, 94–100.e101 (2020).
- Mintzer, J. P. & Moore, J. E. Regional tissue oxygenation monitoring in the neonatal intensive care unit: evidence for clinical strategies and future directions. *Pediatr. Res.* **86**, 296–304 (2019).
- Gilmore, J. H., Knickmeyer, R. C. & Gao, W. Imaging structural and functional brain development in early childhood. *Nat. Rev. Neurosci.* **19**, 123–137 (2018).
- Hansen, M. L. et al. Cerebral near-infrared spectroscopy monitoring versus treatment as usual for extremely preterm infants: a protocol for the SafeBoosC randomised clinical phase III trial. *Trials* **20**, 811 (2019).
- Pichler, G. et al. Reference ranges for regional cerebral tissue oxygen saturation and fractional oxygen extraction in neonates during immediate transition after birth. *J. Pediatr.* **163**, 1558–1563 (2013).
- Mohamed et al. Changes in cerebral tissue oxygenation and fractional oxygen extraction with gestational age and postnatal maturation in preterm infants. *J. Perinatol.* **41**, 836–842 (2021).
- Hyttel-Sorensen et al. Cerebral near-infrared spectroscopy monitoring for prevention of brain injury in very preterm infants. *Cochrane Database Syst. Rev.* **9**, Cd011506 (2017).
- Hyttel-Sorensen et al. A phase II randomized clinical trial on cerebral near-infrared spectroscopy plus a treatment guideline versus treatment as usual for extremely preterm infants during the first three days of life (SafeBoosC): study protocol for a randomized controlled trial. *Trials* **14**, 120 (2013).
- Medtronic. Quick Reference Guide For Premature Neonates. Product Guide. Medtronic. Boulder, CO. (2021).
- Garvey, A. A. & Dempsey, E. M. Applications of near infrared spectroscopy in the neonate. *Curr. Opin. Pediatr.* **30**, 209–215 (2018).
- Dix, L. M. et al. Comparing near-infrared spectroscopy devices and their sensors for monitoring regional cerebral oxygen saturation in the neonate. *Pediatr. Res.* **74**, 557–563 (2013).
- Kamran, M. A., Mannann, M. M. N. & Jeong, M. Y. Differential path-length factor's effect on the characterization of brain's hemodynamic response function: a functional near-infrared study. *Front Neuroinform* **12**, 37 (2018).
- Andresen, B., Greisen, G. & Hyttel-Sorensen, S. Comparison of INVOS 5100C and Nonin SenSmart X-100 oximeter performance in preterm infants with spontaneous apnea. *Pediatr. Res.* **87**, 1244–1250 (2020).
- Zhang, Y. et al. Neonate and infant brain development from birth to 2 years assessed using MRI-based quantitative susceptibility mapping. *Neuroimage* **185**, 349–360 (2019).
- Law, J. B. et al. Intracranial hemorrhage and 2-year neurodevelopmental outcomes in infants born extremely preterm. *J. Pediatr.* **238**, 124–134.e110 (2021).
- Rhee, C. J. et al. Neonatal cerebrovascular autoregulation. *Pediatr. Res.* **84**, 602–610 (2018).
- Covidien. *Operations Manual INVOS® System, Model 5100C* (2013).
- Li, Z. et al. A statistical skull geometry model for children 0–3 years old. *PLoS One* **10**, e0127322 (2015).
- Li, Z. et al. A normative spatiotemporal MRI atlas of the fetal brain for automatic segmentation and analysis of early brain growth. *Sci. Rep.* **7**, 476 (2017).
- Jenkinson, M. et al. FSL. *Neuroimage* **62**, 782–790 (2012).
- Computational Radiology Laboratory at Boston Children's Hospital. (ed. Gholipour, A.) Harvard Fetal Brain Atlas (Boston, MA). (2017).
- Liang, K. Y. & Zeger, S. L. Regression analysis for correlated data. *Annu. Rev. Public Health* **14**, 43–68 (1993).
- R: A Language and Environment for Statistical Computing (R Core Team, 2019).
- Duncan, A. et al. Optical pathlength measurements on adult head, calf and forearm and the head of the newborn infant using phase resolved optical spectroscopy. *Phys. Med. Biol.* **40**, 295–304 (1995).
- Demel, A. et al. Correlation between skin, bone, and cerebrospinal fluid layer thickness and optical coefficients measured by multidistance frequency-domain near-infrared spectroscopy in term and preterm infants. *J. Biomed. Opt.* **19**, 17004 (2014).
- Ostojic, D. et al. Impact of skull thickness on cerebral NIRS oximetry in neonates: an in silico study. *Adv. Exp. Med. Biol.* **1232**, 33–38 (2020).
- Delpy, D. T. et al. Estimation of optical pathlength through tissue from direct time of flight measurement. *Phys. Med. Biol.* **33**, 1433–1442 (1988).
- Jaekel, J. et al. Head growth and intelligence from birth to adulthood in very preterm and term born individuals. *J. Int. Neuropsychol. Soc.* **25**, 48–56 (2019).
- Bushby, K. M. et al. Centiles for adult head circumference. *Arch. Dis. Child* **67**, 1286–1287 (1992).
- Li, T., Gong, H. & Luo, Q. Visualization of light propagation in visible Chinese human head for functional near-infrared spectroscopy. *J. Biomed. Opt.* **16**, 045001 (2011).
- Hoshi, Y. Functional near-infrared spectroscopy: current status and future prospects. *J. Biomed. Opt.* **12**, 062106 (2007).
- Okada, E. et al. Theoretical and experimental investigation of near-infrared light propagation in a model of the adult head. *Appl Opt.* **36**, 21–31 (1997).
- Okada, E. & Delpy, D. T. Near-infrared light propagation in an adult head model. I. Modeling of low-level scattering in the cerebrospinal fluid layer. *Appl Opt.* **42**, 2906–2914 (2003).
- Owen-Reece, H. et al. Near infrared spectroscopy. *Br. J. Anaesth.* **82**, 418–426 (1999).
- Yoshitani, K. et al. Measurements of optical pathlength using phase-resolved spectroscopy in patients undergoing cardiopulmonary bypass. *Anesth. Analg.* **104**, 341–346 (2007).
- Svaasand, L. O. & Ellingsen, R. Optical properties of human brain. *Photochem. Photobiol.* **38**, 293–299 (1983).
- Barkovich, A. J. Magnetic resonance techniques in the assessment of myelin and myelination. *J. Inher. Metab. Dis.* **28**, 311–343 (2005).
- Suppan, E. et al. Three physiological components that influence regional cerebral tissue oxygen saturation. *Front. Pediatr.* **10**, 913223 (2022).
- Kratzer, I., Chip, S. & Vexler, Z. S. Barrier mechanisms in neonatal stroke. *Front. Neurosci.* **8**, 359 (2014).
- Jiang, D. et al. Vessel-specific quantification of neonatal cerebral venous oxygenation. *Magn. Reson. Med.* **82**, 1129–1139 (2019).
- Schwaberg, B. et al. Cerebral blood volume during neonatal transition in term and preterm infants with and without respiratory support. *Front. Pediatr.* **6**, 132 (2018).
- Dawson, J. A. et al. Defining the reference range for oxygen saturation for infants after birth. *Pediatrics* **125**, e1340–e1347 (2010).
- Baytur, Y. B. et al. Assessment of fetal cerebral arterial and venous blood flow before and after vaginal delivery or Cesarean section. *Ultrasound Obstet. Gynecol.* **24**, 522–528 (2004).
- Baik, N. et al. Blood pressure during the immediate neonatal transition: is the mean arterial blood pressure relevant for the cerebral regional oxygenation? *Neonatology* **112**, 97–102 (2017).
- Laurichesse-Delmas, H. et al. Color Doppler study of the venous circulation in the fetal brain and hemodynamic study of the cerebral transverse sinus. *Ultrasound Obstet. Gynecol.* **13**, 34–42 (1999).
- Sood, B. G., McLaughlin, K. & Cortez, J. Near-infrared spectroscopy: applications in neonates. *Semin. Fetal Neonatal Med.* **20**, 164–172 (2015).

52. Baenziger, O. et al. The influence of the timing of cord clamping on postnatal cerebral oxygenation in preterm neonates: a randomized, controlled trial. *Pediatrics* **119**, 455–459 (2007).
53. Tobias, J. D. Assessment of cerebral oxygenation using near infrared spectroscopy during isovolemic hemodilution in pediatric patients. *J. Clin. Monit. Comput.* **25**, 171–174 (2011).
54. Kurth, C. D. & Uher, B. Cerebral hemoglobin and optical pathlength influence near-infrared spectroscopy measurement of cerebral oxygen saturation. *Anesth. Analg.* **84**, 1297–1305 (1997).
55. Zhang, Y. et al. Cerebral near-infrared spectroscopy analysis in preterm infants with intraventricular hemorrhage. *Annu. Int. Conf. IEEE Eng. Med. Biol. Soc.* **2011**, 1937–1940 (2011).
56. Pavlek, L. R. et al. Near-infrared spectroscopy in extremely preterm infants. *Front. Pediatr.* **8**, 624113 (2020).
57. Beausoleil, T. P. et al. Cerebral oxygen saturation and peripheral perfusion in the extremely premature infant with intraventricular and/or pulmonary haemorrhage early in life. *Sci. Rep.* **8**, 6511 (2018).
58. Korček, P. et al. The role of near-infrared spectroscopy monitoring in preterm infants. *J. Perinatol.* **37**, 1070–1077 (2017).
59. Kahn, R. A. & Anyanwu, A. Near-infrared spectroscopy in vegetables and humans: an observational study. *Eur. J. Anaesthesiol.* **35**, 907–910 (2018).

### ACKNOWLEDGEMENTS

We would like to thank the nursing staff at the University of Washington Medical Center in Seattle, Washington, who provided excellent bedside care to the neonates throughout data collection.

### AUTHOR CONTRIBUTIONS

Substantial contributions to the conception and design, acquisition of data, or analysis and interpretation of data: S.E.K., R.M., O.B., J.B.L., N.N., M.D., T.R.W., P.D.M.,

U.M. Drafting the article or revising it critically for important intellectual content: S.E.K., T.R.W., P.M., U.M. Final approval of the version to be published: all authors.

### FUNDING

This research received no specific grant from any funding agency in the public, commercial, or not-for-profit sectors. The study was supported by an internal grant provided by the Division of Child Neurology at Seattle Children's Hospital.

### COMPETING INTERESTS

The authors declare no competing interests.

### ADDITIONAL INFORMATION

**Supplementary information** The online version contains supplementary material available at <https://doi.org/10.1038/s41390-023-02618-x>.

**Correspondence** and requests for materials should be addressed to Sarah E. Kolnik.

**Reprints and permission information** is available at <http://www.nature.com/reprints>

**Publisher's note** Springer Nature remains neutral with regard to jurisdictional claims in published maps and institutional affiliations.

Springer Nature or its licensor (e.g. a society or other partner) holds exclusive rights to this article under a publishing agreement with the author(s) or other rightsholder(s); author self-archiving of the accepted manuscript version of this article is solely governed by the terms of such publishing agreement and applicable law.